DOI: 10.1002/cphc.201200367

Complex Formation of d-Metal Ions at the Interface of Tb^{III}-Doped Silica Nanoparticles as a Basis of Substrate-Responsive Tb^{III}-Centered Luminescence

Nikolay Davydov,[a] Asiya Mustafina,*[a] Vladimir Burilov,[b] Elena Zvereva,[a] Sergey Katsyuba,[a] Liliya Vagapova,[a] Alexander Konovalov,[a] and Igor Antipin[b]

The complex formation of d-metal ions at the interface of Tb^{III}-doped silica nanoparticles modified by amino groups is introduced as a route to sensing d-metal ions and some organic molecules. Diverse modes of surface modification (covalent and noncovalent) are used to fix amino groups onto the silica surface. The interfacial binding of d-metal ions and complexes is the reason for the Tb^{III}-centered luminescence quenching. The regularities and mechanisms of quenching are estimated for the series of d-metal ions and their complexes with chelating ligands. The obtained results reveal the interfacial binding of Cu^{II} ions as the basis of their quantitative determination in the concentration range 0.1–2.5 μM by means of steady-state and time-resolved fluorescence measurements. The variation of chelating ligands results in a significant effect on the quenching regularities due to diverse binding modes (inner or outer sphere) between amino groups at the interface of nanoparticles and Fe^{III} ions. The applicability of the steady-state and time-resolved fluorescence measurements to sense both Fe^{III} ions and catechols in aqueous solution by means of Tb^{III}-doped silica nanoparticles is also introduced.

1. Introduction

Coordination compounds play a significant role in the development of nanomaterials with imaging, sensing, or drug-delivery functions, which are topics of current interest.[1–22] The stimuli responsiveness of the nanomaterial is a required condition of its functionality. Luminescent lanthanide complexes are widely applied in the synthesis of luminescent nanoparticles for imaging and sensing,[5–22] though the principles and mechanisms underlying the development of lanthanide-based stimuli-responsive colloids are not highlighted in the literature. Herein, the main correlations between binding at the interface of lanthanide-based nanoparticles and their luminescence response are introduced for further development of colloids with a sensing function.

Thus, previously reported highly luminescent silica-coated Tb^{III} complexes are chosen as the basis for further development of stimuli-responsive colloids.[6] These nanoparticles exhibit stable luminescence in aqueous solutions due to the poor leakage of the Tb^{III} complex from colloids.[6] The biocompatibility of silica nanoparticles (SNs) results from both the deep encapsulation of hazardous lanthanide complexes into the silica matrix and surface decoration of the nanoparticles. The decoration of the silica surface of nanoparticles by amino groups is a well-known way to modify their cell permeability or affinity to biotargets.[23] The affinity of amino groups towards d-metal ions is also worth noting, since it is widely applied in the sensing or recovery of the latter.[24–27] The quenching effect of d-metal ions on Eu^{III}- and Tb^{III}-centered luminescence is a well-known basis to sense d-metal ions by means of the fluorescence response.[28–32] In our previous work, the adsorption of d-metal ions by unmodified luminescent Tb^{III}-doped SNs followed by their removal from the surface by chelating anions provided a way to sense the latter.[33] The adsorption of d-metal ions by an unmodified silica surface suffers from some shortcomings, which prompted us to apply coordination bonds with some donor groups to bind d-metal ions at the nanoparticles' interface. The reversibility of coordination bonds and the easy shift of the complex formation equilibrium by external stimuli is another advantage. Thus, the affinity of amino groups towards d-metal ions and protons is the reason for their choice for the surface decoration of Tb^{III}-doped SNs. Two types of surface decoration by amino groups are presented herein. The first is based on noncovalent adsorption of polyethyleneimine (PEI) molecules onto the silica surface. The second is the covalent decoration of SNs by 3-[2-(2-aminoethylamino)ethylamino]propyltrimethoxysilane (AEPTS). This work presents the effect of the surface decoration mode (covalent or noncovalent) on the applicability of Tb^{III}-doped SNs to sense d-metal ions through the quenching of Tb^{III}-centered luminescence. The contributions of dynamic and static mechanisms of Tb^{III}-centered luminescence quenching by various d-metal ions are estimated. The significant effect of the ad-

[a] N. Davydov, Dr. A. Mustafina, Dr. E. Zvereva, Prof. S. Katsyuba, Dr. L. Vagapova, Prof. A. Konovalov
A.E. Arbuzov Institute of Organic and Physical Chemistry
Arbuzov Street 8, Kazan (Russia)
Fax: (+7) 8432732253
E-mail: asiyamust@mail.ru

[b] Dr. V. Burilov, Dr. I. Antipin
Kazan (Volga Region) Federal University
Kremlevskaya Street 18, Kazan (Russia)

Supporting information for this article is available on the WWW under http://dx.doi.org/10.1002/cphc.201200367.

ditional ligands on the quenching of Tb^{III}-centered luminescence by d-metal ions is also discussed. The revealed regularities highlight the correlation between interfacial complex formation and the luminescence properties of Tb^{III}-doped SNs as a basis of their sensing function.

2. Results and Discussion

2.1. Synthesis and Surface Modification of Tb^{III}-Doped SNs

The previously reported luminescent SNs ((40 ± 5) nm in size) doped with Tb^{III} complex have been used for noncovalent surface decoration by PEI.[6] The adsorption of PEI molecules onto the silica surface (see the Experimental Section for details) is revealed from the electrokinetic potential measurements (Figure 1). The acidification of colloids of SNs decorated by PEI (SN/PEI) to pH < 5 results in their recharging from −40 to +40 mV, whereas no recharging is possible for the unmodified SNs.

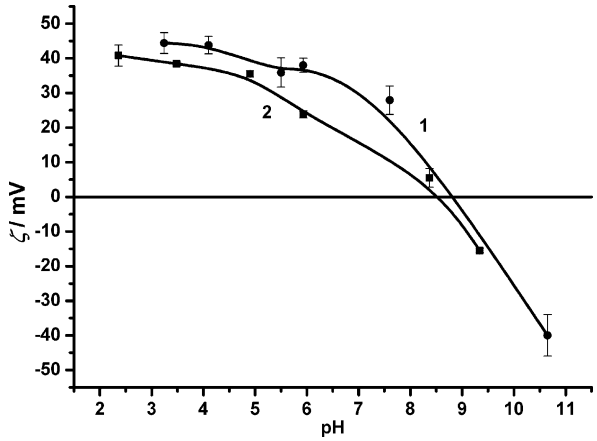

Figure 1. Electrokinetic potential (ζ, mV) of Tb-doped SN/AEPTS (1) and SN/PEI (2) colloids (0.028 g L^{-1}) at various pH values.

The covalent fixing of amino groups onto the silica surface was carried out by means of AEPTS.[23] The size of the obtained nanoparticles is (32 ± 3) nm according to their TEM image (Figure 2). The efficiency of the covalent surface decoration of Tb^{III}-doped SNs by AEPTS was confirmed by quantitative fluorescence analysis.[34] The fluorescence measurements (Figure 1S, Supporting Information) of SNs decorated by AEPTS (SN/AEPTS) reveal about 3 moles of amino groups per 0.1 g of SNs. Taking into account that 0.1 g L^{-1} corresponds to 10^{-8} M of SNs (ref. [6] presents the relation between these values), each SN is decorated by nearly 3000 amino groups.

IR spectroscopy data confirm the presence of amino groups at the surfaces of both SN/PEI and SN/AEPTS colloids (Figures 3 and 4, respectively). The IR spectra of the SNs without surface decoration (curve 1) show a broad band at 3366 cm^{-1} corresponding to O–H stretching. The weak band at 1630 cm^{-1} is assigned to the bending vibrations of water (δH_2O). The IR spectra of the decorated SNs (curve 2) show bands at 3363/3304 and 3351/3300 cm^{-1} originating from NH_2 and NH stretching vibrations of the AEPTS and PEI moieties.[35] It should be mentioned that usually most primary amines give rise to a strong IR band of bending vibrations δNH_2, which can be seen in the IR spectra of AEPTS and SN/AEPTS at 1593 and

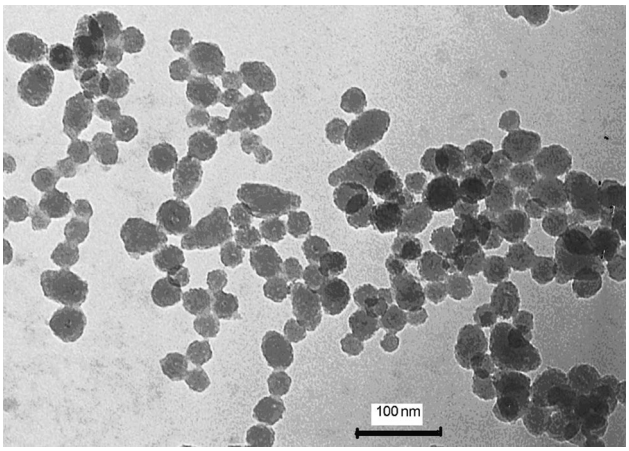

Figure 2. TEM image of SN/AEPTS.

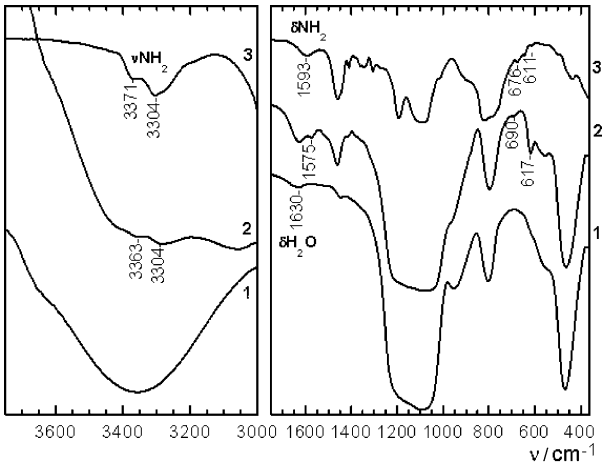

Figure 3. IR spectra of SNs (1), AEPTS-coated SNs (2), and AEPTS (3).

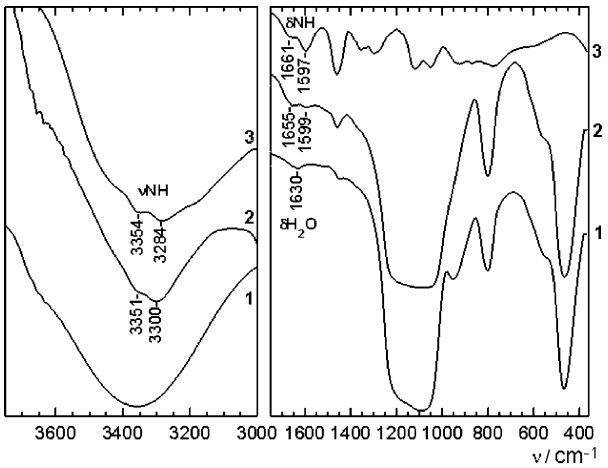

Figure 4. IR spectra of SNs (1), PEI-coated SNs (2), and PEI (3).

1575 cm^{-1} (Figure 3, curves 3 and 2, respectively).[36] Contrary to this, the bending NH vibrations of the secondary aliphatic amines are usually too weak to be observed in routine measurements. Therefore, these vibrations are not registered in the IR spectra of AEPTS and SN/AEPTS, but they are clearly seen in the IR spectra of PEI and SN/PEI (at 1661/1597 and 1655/1599 cm^{-1}) because of the much larger number of NH groups (Figure 4, curves 3 and 2, respectively). The observed shifts of the mentioned bands of stretching and bending modes in the spectra of the decorated SNs relative to the spectra of AEPTS and PEI suggest interactions between the functional groups and surfaces of the nanoparticles.

Electrokinetic potential measurements also reveal the recharging of SN/AEPTS colloids with the acidification of the solution (Figure 1). Moreover, the curve ζ versus pH for SN/AEPTS colloids lies above the similar curve for SN/PEI, thus indicating more protonated amino groups on the surface of SN/AEPTS colloids in comparison with SN/PEI (Figure 1).

2.2. Quenching of SN/PEI and SN/AEPTS Colloids in Solutions of d-Metal Ions

The choice of pH conditions for fluorescence measurements at various concentrations of d-metal ions is influenced by two factors. The first is to keep the pH at a level where the hydrolysis of d-metal ions is insignificant. The second is to maintain the emission intensity at a rather high and constant level, since both silica-coated and "free" Tb^{III} complexes in aqueous solutions are pH dependent.[6,37] Thus, the emission spectra of both SN/PEI and SN/AEPTS colloids were measured at pH values varying from 4 to 9. The emission spectrum of nanoparticles reveals four bands peculiar to the Tb-centered luminescence, with the main peak at 541 nm assigned as the $^5D_4$–$^7F_5$ transition.[6,37] The emission and excitation spectra of SN/AEPTS and SN/PEI colloids are presented in Figure 5. The intensity of the main band at 541 nm was taken as the Tb^{III}-centered emission intensity. The results in Figure 6 exemplify the emission intensity versus pH for SN/AEPTS. Taking into account that alkaline conditions are undesirable due to hydrolysis of d-metal ions and that the emission intensity remains at a constant and significant level at pH 5–7 (Figure 6), the pH was adjusted to 6 by Tris buffer in all measurements.

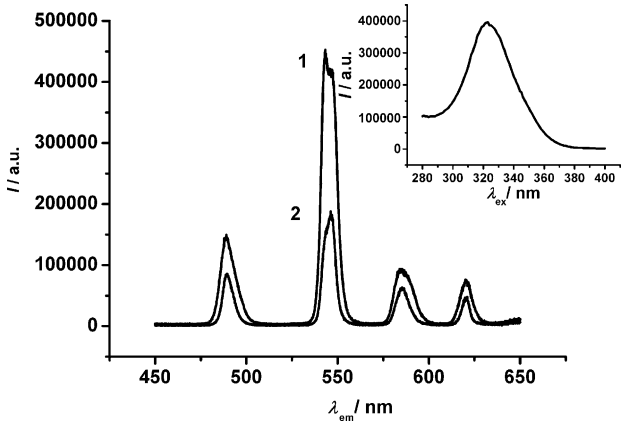

Figure 5. Emission spectra of SN/AEPTS (1) and SN/PEI (2) colloids (0.028 g L^{-1}). The corresponding excitation spectrum is shown in the inset.

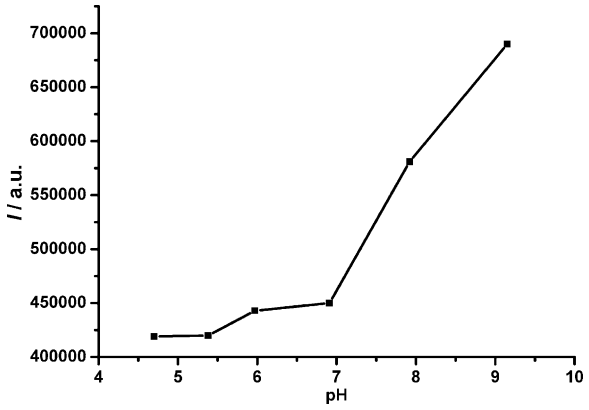

Figure 6. Intensity of the band at 541 nm of SN/AEPTS nanoparticles (0.028 g L^{-1}) at various pH values.

Both steady-state and time-resolved quenching measurements were performed in colloids of SN/PEI and SN/AEPTS at various concentrations of d-metal ions. The quenching measurements are presented in the form of I/I_0 and τ/τ_0, where I and τ are the emission intensity and lifetime values, respectively, of SN/PEI and SN/AEPTS colloids in solutions of d-metal salts of various concentrations, and I_0 and τ_0 are the corresponding values of the initial colloids without d-metal ions (Figures 7 and 8). This mode of presentation enables evaluation of the extent of the quenched luminophores within the SNs. The latter value is of particular importance for SNs doped with luminophores, where the distance between the luminophores and interfacial quenching molecules varies in a rather wide range.[6,33,38] The analysis of the presented data (Figures 7 and 8) should be preceded by the definition of the probable mechanisms of quenching of lanthanide-centered luminescence by d-metal complexes. The dynamic mechanism arising from the donor–acceptor energy transfer and the static mechanism resulting from the ion displacement are the most probable reasons for the lanthanide-centered luminescence quenching by d-metal ions.[28–32] The efficiency of the energy transfer depends on both the distance between luminescent and quenching molecules and the spectral properties of the latter.[39,40] The contribution of the dynamic quenching mechanism revealed from the time-resolved quenching measurements is more significant for SN/AEPTS (Figure 8b) than for SN/PEI (Figure 7b) and highly dependent on the d-metal ion. In particular, the slope of τ/τ_0 versus concentration is the steepest for $CuSO_4$ with a saturation level at 20 μM of $CuSO_4$. No saturation is observed in the case of $FeCl_3$, $FeCl_2$, and $CoCl_2$, while the increase of $MnCl_2$, $NiCl_2$, and $ZnCl_2$ concentrations up to 50 μM induces insignificant changes of both I/I_0 and τ/τ_0 (Figures 7 and 8). It is also worth noting that the saturation levels of τ/τ_0 versus concentration of d-metal ions differ from each other in colloids of SN/PEI and SN/AEPTS. The analysis of these values indicates the greater extent of dynamic quenching in colloids of SN/AEPTS in comparison with SN/PEI, which can be explained by diverse modes of surface modification.

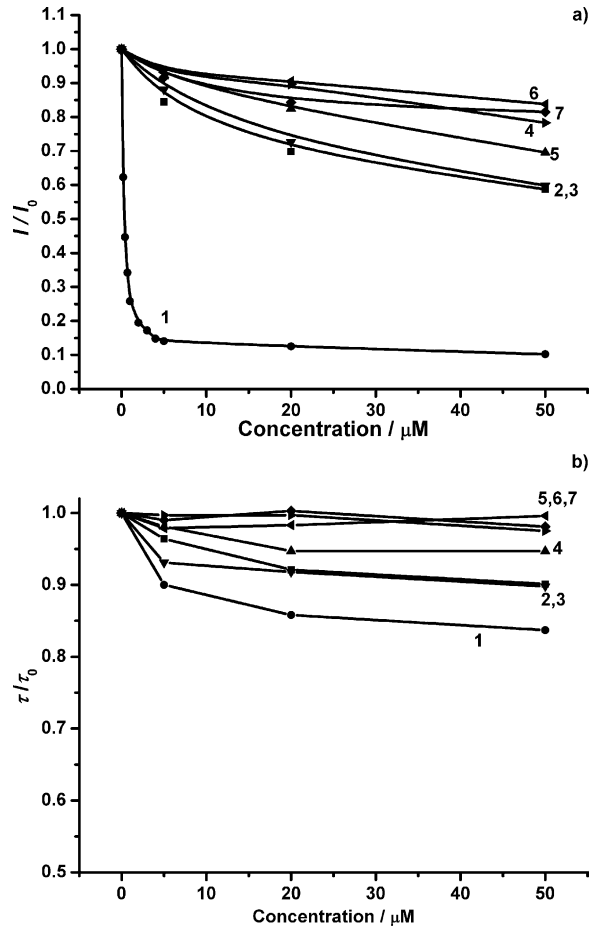

Figure 7. a) I/I_0 and b) τ/τ_0 of SN/PEI colloids (0.028 g L^{-1}) versus concentrations of $CuSO_4$ (1), $FeCl_3$ (2), $CoCl_2$ (3), $FeCl_2$ (4), $NiCl_2$ (5), $ZnCl_2$ (6), and $MnCl_2$ (7) at pH 6.

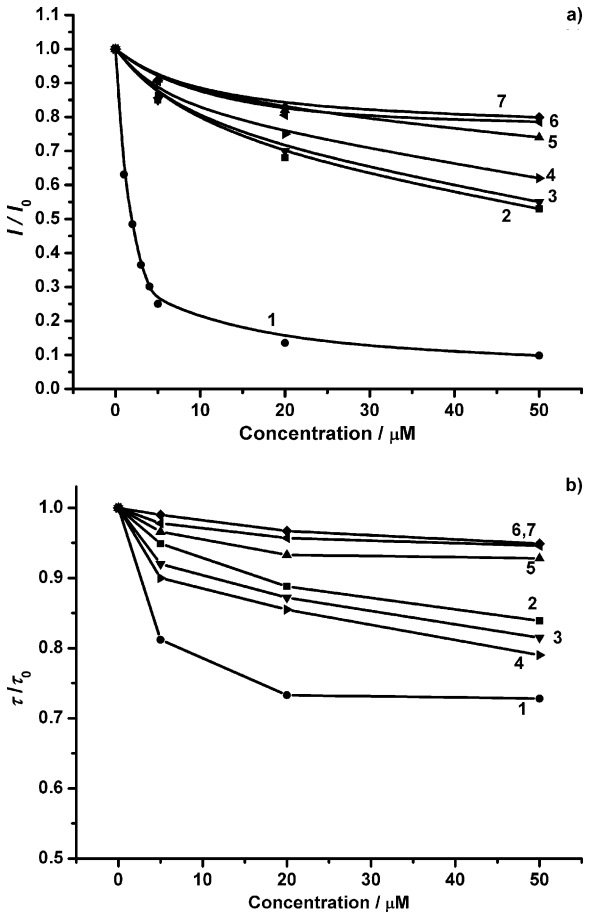

Figure 8. a) I/I_0 and b) τ/τ_0 of SN/AEPTS colloids (0.028 g L^{-1}) versus concentrations of $CuSO_4$ (1), $FeCl_3$ (2), $CoCl_2$ (3), $FeCl_2$ (4), $NiCl_2$ (5), $ZnCl_2$ (6), and $MnCl_2$ (7) at pH 6.

It is anticipated that the quenching measurements should be greatly affected by the distribution of luminophores within the silica matrix. The diverse energy transfer between Tb^{III} luminophores located close to the surface and inside nanoparticles has been demonstrated for the quenching of Tb^{III} luminescence by gold nanoparticles.[41] In our case Tb-doped SNs synthesized through the microemulsion procedure[6] are characterized by the nonhomogeneous distribution of luminophores within SNs, which was designated the "expanded core–shell" morphology, while their further coating by AEPTS makes them closer to the "core–shell" type.[42] The latter type of morphology should provide deeper encapsulation of Tb^{III} complexes into SNs and worse dynamic quenching by interfacial Cu^{II} ions. Nevertheless, both steady-state and time-resolved quenching measurements are in conflict with the above-mentioned assumption, thus indicating more efficient quenching through the dynamic mechanism observed for SN/AEPTS in comparison with SN/PEI colloids (Figure 7b, Figure 8b). This fact can be explained by the bulkiness of the PEI-based adlayer, which in turn restricts the closer proximity of Cu^{II} ions bound with amino groups to silica-coated Tb^{III} complexes. The quenching via a static mechanism is more significant for SN/PEI than for SN/AEPTS, which indicates the enhanced ion displacement of luminescent Tb^{III} by nonluminescent Cu^{II} due to the higher permeability of the PEI adlayer (Figure 7a, Figure 8a). The difference between SN/PEI and SN/AEPTS is observed for other d-metal ions, though it is less pronounced than for $CuSO_4$.

Comparison of the steady-state and time-resolved quenching measurements of SN/PEI and SN/AEPTS colloids in solutions of $FeCl_3$, $FeCl_2$, $CoCl_2$, and $CuSO_4$ reveals Cu^{II} ions as the most efficient quenchers via both dynamic and static mechanisms in comparison with other d-metal ions (Figures 7 and 8). The enhanced interfacial binding of Cu^{II} ions resulting from their greater affinity towards amino groups explains the above-mentioned tendency. Although the displacement of the luminescent Tb^{III} ions by nonluminescent Cu^{II} ions can be assumed as the main reason for the steady-state luminescence quenching, other possible reasons for the decreased emission such as reabsorption or aggregation of SNs should be taken into account.[33] Electrokinetic potential and dynamic light scattering measurements indicate that neither charge neutralization nor aggregation of SN/PEI and SN/AEPTS in the studied solutions is observed (Table 1S, Supporting Information). Reabsorption is also insignificant under such dilute concentration conditions.

Summarizing this issue, it is worth noting that the energy transfer from Tb^{III} complexes to interfacial Cu^{II} ions is more effi-

cient in SN/AEPTS colloids, while static quenching through ion displacement is more enhanced in SN/PEI colloids. The obtained regularities indicate SN/AEPTS colloids to be a more promising basis for the further development of colloids with substrate-responsive luminescence.

2.3. Effect of Additional Ligands on the Quenching Regularities

The binding of metal ions with primary or secondary amino groups of one or two neighboring 3-[2-(2-aminoethylamino)-ethylamino]propyl substituents at the surface of SN/AEPTS is reversible and thus can be schematically introduced by Equilibrium (1):

$$Me + n\,NH_2- \rightleftharpoons Me(NH_2-)_n \quad (1)$$

The admixture of chelating anions is a way to shift Equilibrium (1) due to competitive Equilibriums (2)–(4):

$$Me(NH_2-)_n + L \rightleftharpoons MeL + n\,NH_2- \quad (2)$$

$$Me(NH_2-)_n + L \rightleftharpoons MeL(NH_2-)_n \quad (3)$$

$$Me(L)_m + n\,(NH_3^+) \rightleftharpoons [Me(L)_m](NH_3^+)_n \quad (4)$$

The distance between Tb^{III} complexes and quenching ions is of particular importance in quenching through the dynamic mechanism. Thus, the predominance of Equilibrium (2) should result in removal of metal ions from the nanoparticle interface followed by the fluorescence response. The quenching effect should remain on the same level or even become greater when mixed-ligand complex formation and/or outer-sphere ion pairing [Eqs. (3), (4)] are predominant. The above-mentioned equilibriums indicate that the fluorescence response upon the admixture of various ligands depends on their structure and concentration. Ethylenediaminetetraacetic acid disodium salt (Na_2EDTA) is a well-known chelating ligand, which has found wide application for removing copper and iron ions from their complexes due to the great stability of complexes of Na_2EDTA with d-metal ions.[33,43,44] The series of amino acids (histidine, lysine, glutamic acid, glutamine) can result in diverse effects on the luminescence response due to their tendency to form ternary Cu^{II} complexes with amines [Eq. (3)].[45] The quenching of SN/PEI and SN/AEPTS luminescence by Cu^{II} ions is rather significant and thus the stripping effect of ligands can be applied to provide the luminescence response. Figure 9 presents the I/I_0 values of SN/AEPTS colloids resulting from binding with Cu^{II} ions at 5 μM of $CuSO_4$ and the change of these values upon the addition of diverse amounts of Na_2EDTA. The I/I_0 values increase with the increase of the Na_2EDTA concentration in the range 0–20 μM up to the saturation level, whereas they remain unchanged on the addition of amino acids to SN/AEPTS colloids at 5 μM of $CuSO_4$. These facts indicate that Na_2EDTA provides the fluorescence response of SN/AEPTS, while amino acids do not. The fluorescence response of SN/AEPTS at 5 μM of $CuSO_4$ on Na_2EDTA arises from the reestablished Tb^{III}-centered emission due to the removal of

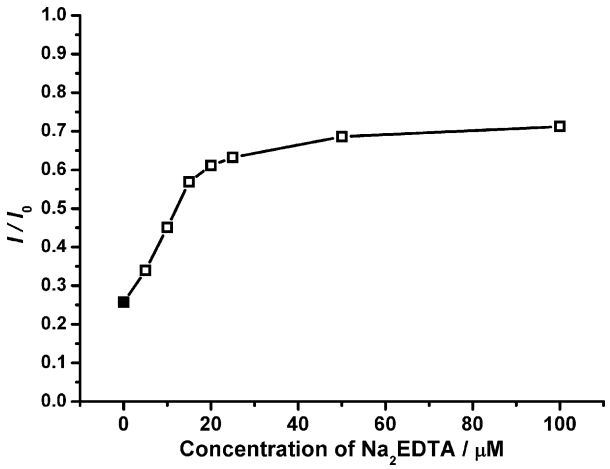

Figure 9. I/I_0 of SN/AEPTS colloids (0.028 g L^{-1}) versus concentration of Na_2EDTA at 5 μM of $CuSO_4$ at pH 6. The I/I_0 values on the addition of amino acids (5–50 μM) are designated by the single filled square.

Cu^{II} ions from the interface of SN/AEPTS resulting from the chelation with Na_2EDTA. The lack of luminescence response on the admixture of amino acids indicates that no stripping of Cu^{II} ions occurs in this case. The predominant contribution of Equilibrium (3) can be assumed to be the explanation of the observed results. The fluorescence responses of SN/PEI colloids differ significantly from those observed for SN/AEPTS. The lack of a fluorescence response on the admixture of both Na_2EDTA and amino acids to SN/PEI colloids confirms the worse stimuli responsiveness of their luminescence than that of SN/AEPTS.

It is worth noting that the increase of I/I_0 values of SN/AEPTS colloids at 5 μM of $CuSO_4$ induced by Na_2EDTA comes to 0.7, while no further growth is observed (Figure 9). This fact confirms the above-mentioned assumption that some luminophores within SN/AEPTS are irreversibly quenched by Cu^{II} ions through ion displacement. Taking into account that the adsorption of small ions into a silica matrix is diffusion controlled,[33,38] the quenching of SN/AEPTS by Cu^{II} ions should be time dependent. Indeed, the I/I_0 values of SN/AEPTS colloids at 1 and 5 μM of $CuSO_4$ decrease within 15 min (Figure 2S, Supporting Information). The increase of I/I_0 values induced by the admixture of Na_2EDTA remains practically unchanged when Na_2EDTA is added immediately after $CuSO_4$ or within 15 min (Figure 2S). So, although Cu^{II} ions provide the most efficient quenching through a dynamic mechanism, the significant contribution of the static mechanism resulting from ion displacement restricts the application of Cu^{II} ions as the quenchers in the development of substrate-responsive luminescent colloids. Nevertheless, the sharp and linear decrease of the emission intensity (Figures 7 and 8) makes SN/PEI and SN/AEPTS colloids rather promising for the detection of Cu^{II} ions under rather dilute conditions (0–2.5 μM). For example, the lower detection level (0.1 μM) and linear range (0.1–2.5 μM) of the Cu^{II} sensing by SN/PEI and SN/AEPTS are comparable with similar values obtained by the use of quantum dots.[46,47]

The contributions of both static and dynamic mechanisms of SN/AEPTS quenching in solutions of $FeCl_3$ are less significant in comparison with $CuSO_4$. This fact agrees well with the less

efficient binding of amino groups with Fe^{III} ions[25] and their tendency to hydrolysis. Concentrated conditions are required to obtain a more or less significant fluorescence response on the stripping effect of Na_2EDTA. For example, 20 μM of $FeCl_3$ is required to decrease I/I_0 from 1 to 0.7, while 60 μM of Na_2EDTA should be added for reestablishment of the emission intensity to 0.9. Thus, the admixture of an additional ligand can be applied to enhance the quenching effect of Fe^{III} ions on the Tb-centered luminescence of SN/AEPTS.

The binding of quenchers via outer-sphere ion pairing at the interface of SN/AEPTS according to Equilibrium (4) is exemplified by the quenching measurements of SN/AEPTS in solutions of $K_3[Fe(CN)_6]$ and $K_4[Fe(CN)_6]$ (Figure 10). The decrease of both I/I_0 and τ/τ_0 occurs in a more narrow concentration range than that observed for Fe^{III} ions (Figures 8 and 10), thus indicating that the electrostatic attraction of $[Fe(CN)_6]^{3-}$ and $[Fe(CN)_6]^{4-}$

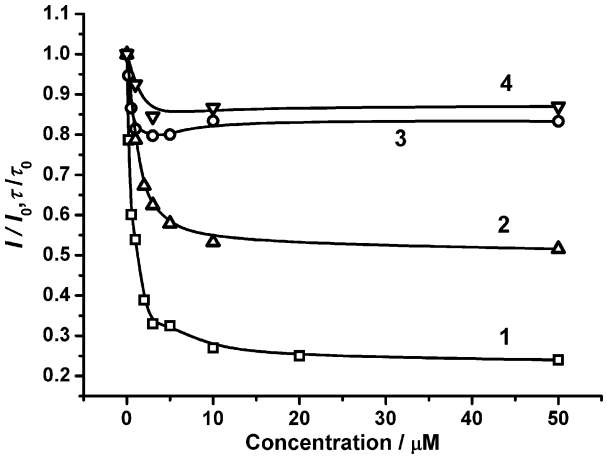

Figure 10. I/I_0 (1,2) and τ/τ_0 (3,4) of SN/AEPTS colloids (0.028 g L^{-1}) versus concentrations of $K_3[Fe(CN)_6]$ (1,3) and $K_4[Fe(CN)_6]$ (2,4) at pH 6.

anions to protonated amino groups provides more efficient binding of the quenching ions than the coordination of Fe^{III} ions via amino groups at the surface of SN/AEPTS. The above results reveal outer-sphere ion pairing as a convenient mode of interfacial binding with quenching ions. The significant contribution of the static mechanism to the quenching by $K_3[Fe(CN)_6]$ should be noted as a shortcoming. The ion pairing between Tb^{3+} and $[Fe(CN)_6]^{3-}$ is the probable explanation of the enhanced decrease of the steady-state Tb-centered luminescence in solutions of $K_3[Fe(CN)_6]$.

The choice of 1,2-dihydroxybenzene (H_2DB) and Tiron (Na_2H_2T) as the additional ligands has been conditioned by their complex formation with Fe^{III}, which results in negatively charged $[Fe(DB)_2]^-$ and $[Fe(DB)_3]^{3-}$, as well as $[Fe(T)_2]^{-5}$ and $[Fe(T)_3]^{-9}$ at pH 6 and excess amounts of 1,2-dihydroxybenzene and Tiron.[48,49] Moreover, these complexes have absorption bands at 500–700 nm, overlapping with the emission bands of Tb^{III}, which can be assumed as a prerequisite for quenching through the energy-transfer mechanism and/or the inner filter effect.[50] It is also worth noting that 1,2-dihydroxybenzene is the simplest representative of catechol-containing molecules. These molecules are of widespread biological occurrence and importance due to their function as neurotransmitters and their pharmacological use in the treatment of Parkinson's disease, hypertension, and breast cancer.[51,52]

Comparison of the quenching measurements in SN/AEPTS colloids by $FeCl_3$ in the absence and the presence of 1,2-dihydroxybenzene at the same pH value reveals the effect of 1,2-dihydroxybenzene on the quenching regularities (Figure 8 and 11). First of all the decrease of both τ/τ_0 and I/I_0 becomes more sharp, thereby indicating that 1,2-dihydroxybenzene enhances

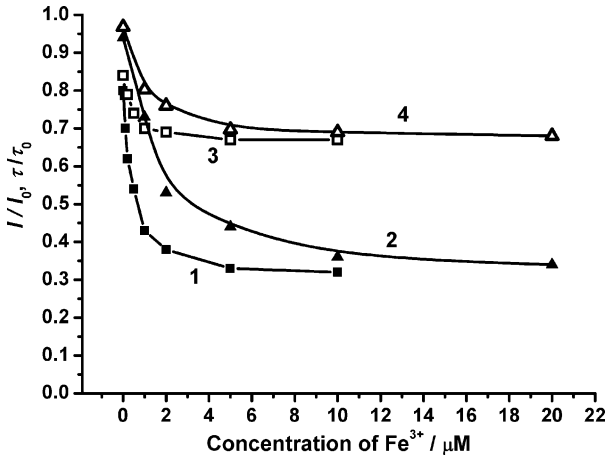

Figure 11. I/I_0 (1,2) and τ/τ_0 (3,4) of SN/AEPTS colloids (0.028 g L^{-1}) versus concentration of $FeCl_3$ at 2 μM of Tiron (1,3) and 10 μM of 1,2-dihydroxybenzene (2,4) at pH 6.

the binding of Fe^{III} ions with SN/AEPTS. The formation of $[Fe(DB)_2]^-$ and $[Fe(DB)_3]^{3-}$, which can be ion paired with the protonated amino groups, explains the rather sharp decrease of τ/τ_0 and I/I_0 in the narrow concentration range of Fe^{III} (0–2.5 μM). So, the admixture of 1,2-dihydroxybenzene enables the detection limit of the sensing of $FeCl_3$ by SN/AEPTS colloids to be decreased to 0.2 μM. The outer-sphere ion pairing of quenching complexes with protonated amino groups is the main reason for the above-mentioned tendency. Thus, it is anticipated that complexes $[Fe(T)_2]^{-5}$ and $[Fe(T)_3]^{-9}$ should provide the quenching under more dilute conditions than the less negatively charged $[Fe(DB)_2]^-$ and $[Fe(DB)_3]^{3-}$ due to their enhanced electrostatic attraction with the protonated amino groups. Moreover, UV/Vis spectroscopy data in the literature reveal the shift of the equilibrium between $[Fe(T)_2]^{-5}$ and $[Fe(T)_3]^{-9}$ towards the latter in the presence of cationic surfactants.[53] The intensities of the absorption bands are too small under the studied concentration conditions to reveal such a shift. Also note that the inner filter effect of these Fe^{III} complexes is insignificant under such dilute conditions.

The data presented in Figure 11 indicate that the lower detection limit of Fe^{III} can be decreased from 0.2 to 0.04 μM when Tiron is added instead of 1,2-dihydroxybenzene. The charge of the additional ligand increases the slopes of τ/τ_0 and I/I_0 versus concentration of $FeCl_3$, while the saturation levels are the same in both cases (Figure 11).

It is also anticipated that the quenching effect of $FeCl_3$ on the Tb^{III}-centered luminescence of SN/AEPTS colloids should be enhanced by the addition of 1,2-dihydroxybenzene or Tiron. Figure 12 presents the steady-state and time-resolved quenching at various concentrations of 1,2-dihydroxybenzene and Tiron and constant concentrations of $FeCl_3$. The insignificant quenching resulting from 1 μM of $FeCl_3$ can be greatly enhanced at 0.05 μM of Tiron with a further linear decrease within its concentration range of 0.05–2 μM. The insignificant effect of 1,2-dihydroxybenzene was revealed under the same concentration conditions. The quenching effect of 1,2-dihydroxybenzene becomes detectable at 5 μM of $FeCl_3$, though no saturation of τ/τ_0 and I/I_0 values is observed within the studied concentration range (0–20 μM) of 1,2-dihydroxybenzene (Figure 12).

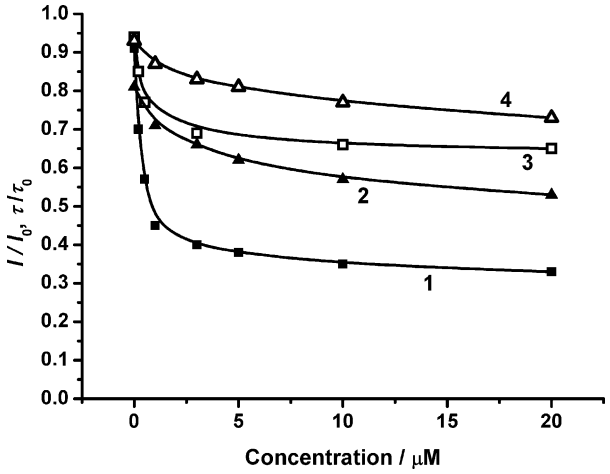

Figure 12. I/I_0 (1,2) and τ/τ_0 (3,4) of SN/AEPTS colloids (0.028 g L^{-1}) versus concentrations of Tiron at 1 μM of $FeCl_3$ (1,3) and 1,2-dihydroxybenzene at 5 μM of $FeCl_3$ (2,4) at pH 6.

3. Conclusions

Summarizing the obtained results, the following points are worth noting:

1. The steady-state and time-resolved luminescence of silica-coated Tb complexes is quenched by d-metal ions bound with amino groups at the silica/water interface. The quenching occurs via both dynamic and static mechanisms. The mode of the silica surface decoration by amino groups greatly affects the relative importance of the dynamic and static mechanisms. Dynamic quenching is more significant for nanoparticles with covalent decoration by AEPTS in comparison with those decorated through the adsorption of PEI.

2. The steady-state and time-resolved quenching measurements of SN/AEPTS in solutions of d-metal salts, introduced in the form of I/I_0 and τ/τ_0, open the route to detect Cu^{II} ions with a lower detection level and dynamic linear range of 0.1 μM and 0.1–2.5 μM, respectively. The enhanced affinity of Cu^{II} ions towards amino groups is the reason for the most efficient quenching of SN/AEPTS in solutions of $CuSO_4$.

3. The quenching regularities can be modified by tuning of the interaction mode between the quenching ions and Tb^{III}-doped SN/AEPTS. The outer-sphere ion pairing of the charged Fe^{III} complexes with the protonated amino groups of SN/AEPTS provides more efficient quenching than the inner-sphere coordination of Fe^{III} ions with amino groups. Thus, the quenching effect of Fe^{III} ions can be significantly reinforced by the addition of 1,2-dihydroxybenzene and Tiron, and vice versa catechol derivatives enhance the quenching of the Tb-centered luminescence in the presence of Fe^{III} ions. Moreover, the anionic substituents in the aromatic rings of catechol derivatives greatly affect the quenching regularities. These results highlight the tuning of the interfacial binding mode of d-metal ions from inner to outer sphere as a route to obtain substrate-responsive luminescent colloids.

Experimental Section

Transmission electron microscopy (TEM) images were obtained using a JEOL JEM 100 S microscope (JEOL, Japan).

Dynamic light scattering measurements and zeta-potential values of nanoparticles in aqueous dispersions were analyzed using a Malvern Mastersize 2000 particle analyzer.

The steady-state emission spectra were recorded on a spectrofluorometer FL3-221-NIR (Jobin Yvon) under 330 nm excitation.

Luminescence decay measurements were performed using a Horiba Jobin Yvon Fluorolog 3-221 spectrofluorometer with SPEX FL-1042 phosphorimeter accessory using a xenon flash lamp as the photon source with the following parameters: time per flash: 50.00 ms, flash count: 200 ms, initial delay: 0.05 ms, and sample window: 2 ms. Excitation of samples was performed at 330 nm and emission was detected at 546 nm with a 5 nm slit width for both excitation and emission.

UV/Vis spectra were recorded on a Lambda 35 spectrophotometer (PerkinElmer).

IR spectra of all compounds were recorded on a FTIR spectrometer "Tensor 27" (Bruker) in the 4000–400 cm^{-1} mid-IR range at an optical resolution of 1 cm^{-1}. The liquid samples of AEPTS or PEI were placed between KBr plates. Dry powders of nanoparticles obtained from their water solutions were prepared as KBr pellets and heated to over 100 °C to remove traces of water.

Tetraethyl orthosilicate (TEOS, 98%), 3-[2-(2-aminoethylamino)ethylamino]propyltrimethoxysilane (AEPTS, 98%), ammonium hydroxide (28–30%), *n*-heptanol (98%), and cyclohexane (99%) were from Acros; terbium(III) nitrate hexahydrate (99.9%) from Alfa Aesar and Triton X-100 from Sigma–Aldrich were used. The synthesis of *p*-sulfonatothiacalix[4]arene (TCAS) was carried out according to the known procedure.[54] Na_2EDTA, Tiron (4,5-dihydroxybenzene-1,3-disulfoacid disodium salt), $FeCl_3{\cdot}6H_2O$, $FeCl_2{\cdot}6H_2O$, $NiCl_2{\cdot}6H_2O$, $MnCl_2{\cdot}4H_2O$, $CoCl_2{\cdot}6H_2O$, $CuSO_4{\cdot}5H_2O$, $ZnCl_2{\cdot}4H_2O$, $K_4[Fe(CN)_6]{\cdot}3H_2O$, $K_3[Fe(CN)_6]$, and PEI were used as purchased from Acros. 1,2-Dihydroxybenzene was purified by recrystallization from benzene prior to use (m.p. 105 °C).

The synthesis of silica-coated Tb-TCAS nanoparticles was performed according to a reverse microemulsion procedure.[6] The nanoparticles were characterized by transmission microscopy (Figure 3S, Supporting Information).

The noncovalent decoration of silica-coated Tb-TCAS nanoparticles resulted from the adsorption of PEI onto SNs. An aqueous dispersion of Tb-doped SNs (4 g L^{-1}) was mixed with an aqueous solution of PEI (2 g L^{-1}) with further stirring and ultrasonication. The nanoparticles with adsorbed PEI were precipitated by centrifugation. The washing of PEI-modified SNs was performed several times

through the redispersion of nanoparticles in water followed by their precipitation.

The synthesis of Tb-doped SNs covalently decorated by amino groups was performed with the use of AEPTS in accordance with the known procedure.[23] An aqueous solution of luminescent complex Tb-TCAS (0.0078 M) was added dropwise to a mixture of Triton X-100 (4.315 g), cyclohexane (16.75 mL), and *n*-hexanole (4.05 mL) with stirring for 15 min. Then aqueous ammonia (30%) was added (0.135 mL) to the mixture. After stirring for 15 min, TEOS (0.133 mL) was added and the reaction was continued for 24 h. Then TEOS (0.133 mL) was added to the mixture, followed by the addition of AEPTS (0.023 mL) 30 min later. The reaction continued for another 24 h. To remove the remaining surfactants, the SNs were centrifuged at 4000 rpm and washed with acetone/ethanol (1:1), ethanol, and water several times.

The quantitative analysis of amino groups on the surface of Tb-doped SNs modified by AEPTS was carried out by a fluorescence procedure with the use of fluorescamine.[34] Alanine solutions in the concentration range 0.408–5.37 μM were used to make the calibration curve. Excitation of samples was performed at 390 nm, and emission was detected at 490 nm with a 2 nm slit width for both excitation and emission.

All samples were prepared from bidistilled water with prior filtering through a PVDF membrane using a syringe filter (0.45 μm). All samples were ultrasonicated within 30 min before measurements. All measurements were performed triply at least.

Acknowledgements

We thank Dr I. I. Vandykova for help in IR measurements and RFBR (No. 10-03-00352) for financial support.

Keywords: colloids · transition metals · luminescence · nanoparticles · sensors

[1] M.-J. Li, Z. Chen, V. W.-W. Yam, Y. Zu, *ACS Nano* **2008**, *2*, 905 – 912.
[2] S. Santra, R. P. Bagwe, D. Dutta, J. T. Stanley, G. A. Walter, W. Tan, B. M. Moudgil, R. A. Mericle, *Adv. Mater.* **2005**, *17*, 2165 – 2169.
[3] L. Wang, K. Wang, S. Santra, X. Zhao, L. R. Hilliard, J. E. Smith, Y. Wu, W. Tan, *Anal. Chem.* **2006**, *78*, 646 – 654.
[4] H. Wu, Q. Huo, S. Varnum, J. Wang, G. Liu, Z. Nie, J. Liu, Y. Lin, *Analyst* **2008**, *133*, 1550 – 1555.
[5] Z. Ye, M. Tan, G. Wang, J. Yuan, *Talanta* **2005**, *65*, 206 – 210.
[6] A. R. Mustafina, S. V. Fedorenko, O. D. Konovalova, A. Yu. Menshikova, N. N. Shevchenko, S. E. Soloveva, A. I. Konovalov, I. S. Antipin, *Langmuir* **2009**, *25*, 3146 – 3151.
[7] F. Enrichi, R. Ricco, P. Scopece, A. Parma, A. R. Mazaheri, P. Riello, A. Benedetti, *J. Nanopart. Res.* **2010**, *12*, 1925 – 1931.
[8] F. Gao, F. Luo, X. Chen, W. Yao, J. Yin, Zh. Yao, L. Wang, *Talanta* **2009**, *80*, 202 – 206.
[9] H. Jiang, G. Wang, W. Zhang, X. Liu, Z. Ye, D. Jin, J. Yuan, Z. Liu, *J. Fluoresc.* **2010**, *20*, 321 – 328.
[10] K. Binnemans, P. Lenaerts, K. Driesen, C. Görller-Walrand, *J. Mater. Chem.* **2004**, *14*, 191 – 195.
[11] C. Wu, J. Hong, X. Guo, C. Huang, J. Lai, J. Zheng, J. Chen, X. Mu, Y. Zhao, *Chem. Commun.* **2008**, 750 – 752.
[12] Y. Wang, Y. Wang, P. Cao, Y. Li, H. Li, *CrystEngComm* **2011**, *13*, 177 – 181.
[13] H. Härmä, C. Graf, P. Hänninen, *J. Nanopart. Res.* **2008**, *10*, 1221 – 1224.
[14] H. Peng, C. Wu, Y. Jiang, S. Huang, J. McNeill, *Langmuir* **2007**, *23*, 1591 – 1595.
[15] P. Yang, M. Ando, N. Murase, *New J. Chem.* **2009**, *33*, 1457 – 1461.
[16] R.-J. Zhang, J.-W. Cui, D.-M. Lu, W.-G. Hou, *Chem. Commun.* **2007**, 1547 – 1549.
[17] J.-W. Cui, R.-J. Zhang, Z.-G. Lin, L. Li, W.-R. Jin, *Dalton Trans.* **2008**, 899.
[18] C. P. Hauser, N. Jagielski, J. Heller, D. Hinderberger, H. W. Spiess, I. Lieberwirth, C. K. Weiss, K. Landfester, *Langmuir* **2011**, *27*, 12859 – 12868.
[19] L. Armelao, S. Quici, F. Barigelletti, G. Accorsic, G. Bottaro, M. Cavazzini, E. Tondello, *Coord. Chem. Rev.* **2010**, *254*, 487 – 505.
[20] C. Tan, Q. Wang, *Inorg. Chem.* **2011**, *50*, 2953 – 2956.
[21] Q. Wang, C. Tan, H. Chen, H. Tamiaki, *J. Phys. Chem. C* **2010**, *114*, 13879 – 13883.
[22] C. Tan, Q. Wang, C. C. Zhang, *Chem. Commun.* **2011**, *47*, 12521 – 12523.
[23] R. P. Bagwe, L. R. Hilliard, W. Tan, *Langmuir* **2006**, *22*, 4357 – 4362.
[24] S. T. Beatty, R. J. Fischer, E. A. Rosenberg, D. Pang, *Sep. Sci. Technol.* **1999**, *34*, 2723 – 2739.
[25] M. Laatikainen, K. Sirola, E. Paatero, *Colloids Surf. A* **2007**, *296*, 191 – 205.
[26] A. Wua, J. Jia, S. Luan, *Colloids Surf. A* **2011**, *384*, 180 – 185.
[27] I. Y. Goon, C. Zhang, M. Lim, J. J. Gooding, R. Amal, *Langmuir* **2010**, *26*, 12247 – 12252.
[28] Q. Wang, C. Tan, *Anal. Chim. Acta* **2011**, *708*, 111 – 115.
[29] B. C. Barja, P. F. Aramendría, *Photochem. Photobiol. Sci.* **2008**, *7*, 1391 – 1399.
[30] B. C. Barja, A. Remorino, M. J. Roberti, P. F. Aramendia, *J. Argent. Chem. Soc.* **2005**, *93*, 81 – 96.
[31] C. Tan, Y. Zheng, Q. Wang, W. Zhang, S. Zheng, S. Cai, *J. Fluoresc.* **2011**, *21*, 1117 – 1122.
[32] M. Turel, A. Duerkop, A. Yegorova, Y. Scripinets, A. Lobnik, N. Samec, *Anal. Chim. Acta* **2009**, *644*, 53 – 60.
[33] V. Skripacheva, A. Mustafina, N. Davydov, V. Burilov, A. Konovalov, S. Soloveva, I. Antipin, *Mater. Chem. Phys.* **2012**, *132*, 488 – 493.
[34] H. Ritter, D. Brühwiler, *J. Phys. Chem. C* **2009**, *113*, 10667 – 10674.
[35] N. B. Colthup, L. H. Daly, S. E. Wiberley, *Introduction to Infrared and Raman Spectroscopy*, Academic Press, New York, **1964**, p. 511.
[36] L. J. Bellamy, *The Infrared Spectra of Complex Molecules*, Methuen, London, **1957**, p. 433.
[37] N. Iki, T. Horiuchi, K. Koyama, N. Morohashi, C. Kabuto, S. Miyano, *J. Chem. Soc. Perkin Trans. 2* **2001**, 2219 – 2225.
[38] "Energy Transfer in Silica Nanoparticles: An Essential Tool for the Amplification of the Fluorescence Signal": S. Bonacchi, D. Genovese, R. Juris, E. Marzocchi, M. Montalti, L. Prodi, E. Rampazzo, N. Zaccheroni in *Reviews in Fluorescence 2008*, Springer, New York, **2010**, pp. 119 – 137.
[39] Th. Förster, *Discuss. Faraday Soc.* **1959**, *27*, 7 – 17.
[40] J. R. Lakowicz, *Principles of Fluorescence Spectroscopy*, Springer, New York, **2006**, p. 954.
[41] J.-Q. Gu, J. Shen, L.-D. Sun, C.-H. Yan, *J. Phys. Chem. C* **2008**, *112*, 6589 – 6593.
[42] D. R. Larson, H. Ow, H. D. Vishwasrao, A. A. Heikal, U. Wiesner, W. W. Webb, *Chem. Mater.* **2008**, *20*, 2677 – 2684.
[43] S. Seo, H. Y. Lee, M. Park, J. M. Lim, D. Kang, J. Yoon, J. H. Jung, *Eur. J. Inorg. Chem.* **2010**, 843 – 847.
[44] G. Bianké, V. Chaurin, M. Egorov, J. Lebreton, E. C. Constable, C. E. Housecroft, R. Häner, *Bioconjugate Chem.* **2006**, *17*, 1441 – 1446.
[45] P. Venkataiah, M. S. Mohan, Y. L. Kumari, *Proc. Indian Acad. Sci. Chem. Sci.* **1992**, *104*, 453 – 456.
[46] B. Dong, L. Cao, G. Su, W. Liu, H. Qu, D. Jiang, *J. Colloid Interface Sci.* **2009**, *339*, 78 – 82.
[47] H. Dong, Y. Liu, D. Wang, W. Zhang, Z. Ye, G. Wang, J. Yuan, *Nanotechnology* **2010**, *21*, 395504.
[48] A. Avdeef, S. R. Sofen, T. L. Bregante, K. N. Raymond, *J. Am. Chem. Soc.* **1978**, *100*, 5362 – 5370.
[49] M. Elhabiri, C. Carrër, F. Marmolle, H. Traboulsi, *Inorg. Chim. Acta* **2007**, *360*, 353 – 359.
[50] M. J. Sever, J. J. Wilker, *Dalton Trans.* **2004**, 1061 – 1072.
[51] S. Arreguin, P. Nelson, S. Padway, M. Shirazi, C. Pierpont, *J. Inorg. Biochem.* **2009**, *103*, 87 – 93.
[52] S. Paria, P. Halder, T. K. Paine, *Inorg. Chem.* **2010**, *49*, 4518 – 4523.
[53] S. N. Bhadani, M. Tiwari, A. Agrawal, C. S. Kavipurapu, *Mikrochim. Acta* **1994**, *117*, 15 – 22.
[54] N. Iki, T. Fujimoto, S. Miyano, *Chem. Lett.* **1998**, 625 – 626.

Received: April 28, 2012
Revised: June 14, 2012
Published online on July 4, 2012

